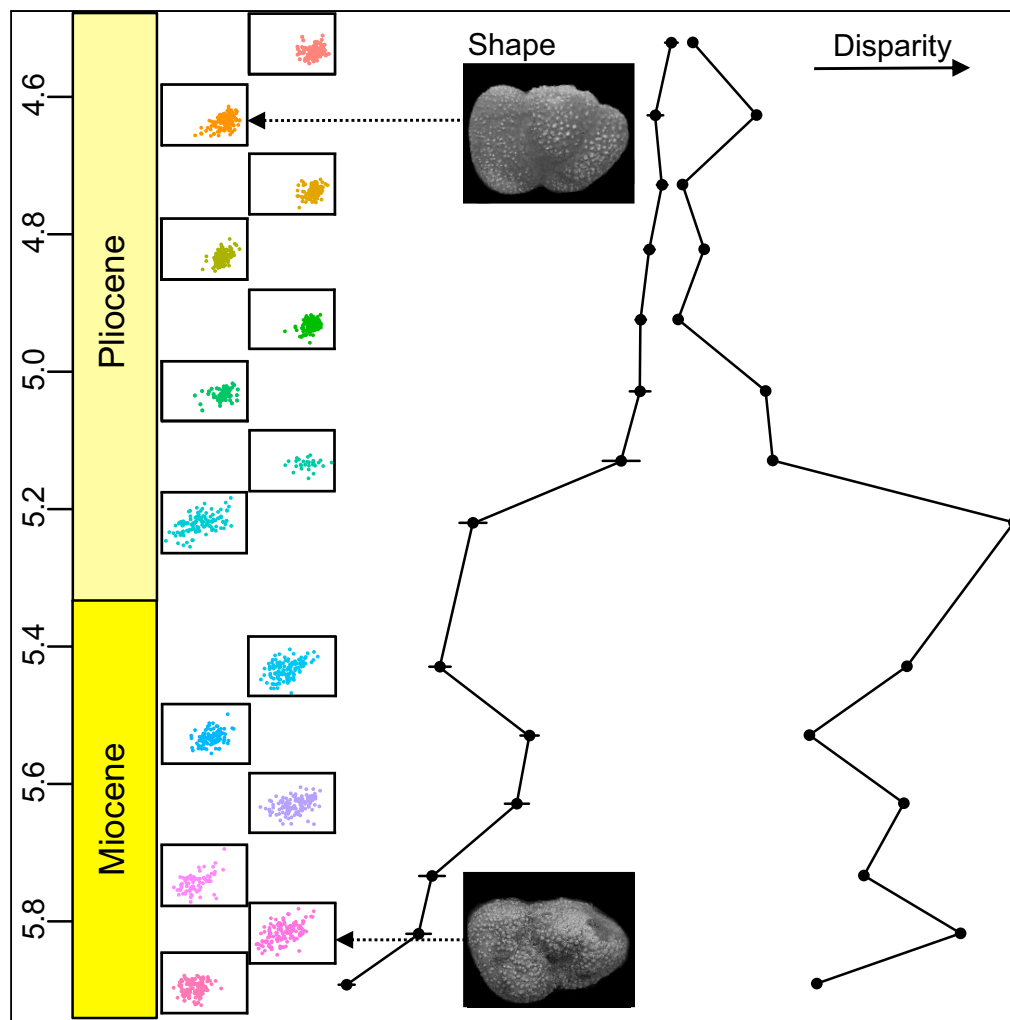


## Article

Evolutionary Transition in the Late Neogene  
Planktonic Foraminiferal Genus *Truncorotalia*

Russell D.C.  
Bicknell, Katie S.  
Collins, Martin  
Crundwell,  
Michael Hannah,  
James S.  
Crampton,  
Nicolás E.  
Campione

rdcbicknell@gmail.com

**HIGHLIGHTS**

Evolution of planktonic  
foraminiferal anatomy  
across Miocene/Pliocene  
boundary

Novel application of  
multivariate analyses to  
1,459 specimens

Evidence for a punctuated  
anatomical shift  
associated with the  
boundary

Bicknell et al., iScience 8, 295–  
303  
October 26, 2018 © 2018 The  
Author(s).  
[https://doi.org/10.1016/  
j.isci.2018.09.013](https://doi.org/10.1016/j.isci.2018.09.013)

## Article

Evolutionary Transition in the Late Neogene Planktonic Foraminiferal Genus *Truncorotalia*

Russell D.C. Bicknell,<sup>1,5,\*</sup> Katie S. Collins,<sup>2</sup> Martin Crundwell,<sup>3</sup> Michael Hannah,<sup>4</sup> James S. Crampton,<sup>3,4</sup> and Nicolás E. Campione<sup>1</sup>

## SUMMARY

The fossil record provides empirical patterns of morphological change through time and is central to the study of the tempo and mode of evolution. Here we apply likelihood-based time-series analyses to the near-continuous fossil record of Neogene planktonic foraminifera and reveal a morphological shift along the *Truncorotalia* lineage. Based on a geometric morphometric dataset of 1,459 specimens, spanning 5.9–4.5 Ma, we recover a shift in the mode of evolution from a disparate latest Miocene morphospace to a highly constrained early Pliocene morphospace. Our recovered dynamics are consistent with those stipulated by Simpson's quantum evolution and Eldredge-Gould's punctuated equilibria and supports previous suppositions that even within a single lineage, evolutionary dynamics require a multi-parameter model framework to describe. We show that foraminiferal lineages are not necessarily gradual and can experience significant and rapid transitions along their evolutionary trajectories and reaffirm the utility of multivariate datasets for their future research.

## INTRODUCTION

Reconstruction of evolutionary patterns, such as gradualism, stasis, quantum evolution (QE), punctuated equilibria (PE), and punctuated anagenesis, have driven generations of evolutionary biologists and palaeontologists to understand the history of life (e.g., Darwin, 1859; Depéret, 1907; Simpson, 1944; Eldredge and Gould, 1972; Gould and Eldredge, 1977; Wei and Kennett, 1988; Hunt, 2006; Hunt et al., 2015). Many fossil groups have been used to document evolutionary trends (see Hunt, 2007). Among them, the planktonic foraminiferal fossil records are recognized as being especially useful for studying the tempo and mode of evolution (Frerichs, 1971; Malmgren et al., 1983; Stanley et al., 1988; Collins, 1989; Hunt, 2006; Ezard et al., 2011; Pearson and Ezard, 2014). Planktonic foraminifera are single-celled marine protists with calcite shells (or tests) that are distributed almost ubiquitously in the ocean (Strotz and Allen, 2013; Hsiang et al., 2016). Tests are structurally robust and easily preserved in hemipelagic sediments and biogenic oozes in the deep sea, which are not typically affected by high rates of erosion (Aze et al., 2011). Under ideal sedimentation conditions, these deposits represent specimen-rich, near-continuous records of deposition (Pearson, 1993; Aze et al., 2011; Lazarus, 2011). The ability to gather large samples of specimens at a high temporal resolution makes deep-sea microfossil records ideal for studying and understanding evolution (Lazarus, 2011).

Neogene planktonic foraminiferal fossil lineages have been used to interpret gradualism (Arnold, 1983; Belyea and Thunell, 1984; Wei, 1987; Wei and Kennett, 1988), PE (Wei and Kennett, 1988), and punctuated anagenesis (Malmgren et al., 1983, 1996). However, the last decade has seen the emergence of sophisticated model-fitting techniques for time series that are ideal tools for testing the evolutionary tempo and mode (Hunt, 2006, 2008; Hunt and Carrano, 2010; Hunt et al., 2015). These advances call for a re-evaluation of the previously interpreted evolutionary patterns, and a consideration of understudied late Neogene lineages, such as *Truncorotalia*, examined here. Recent truncorotalid diversity is related to the evolution of *Truncorotalia crassaformis*, an extant species that arose after the Miocene/Pliocene boundary from a contentious ancestral species (Hornibrook, 1981; Kennett and Srinivasan, 1983; Cifelli and Scott, 1986; Bylinskaya, 2004; Boudagher-Fadel, 2012; Scott et al., 2015). Notably, Arnold (1983) hypothesized a gradual transition from *Truncorotalia juanai* (= *Hirsutella cibaoensis* in Arnold (1983)) toward *T. crassaformis* across the boundary. However, by using semilandmark geometric morphometrics and maximum likelihood-based time-series analyses (Hunt et al., 2015) we reveal an abrupt evolutionary transition along the *Truncorotalia* lineage after the Miocene/Pliocene boundary (Crundwell and Nelson, 2007). Our results therefore

<sup>1</sup>Palaeoscience Research Centre, School of Environmental and Rural Science, University of New England, Armidale 2351, Australia

<sup>2</sup>Department of the Geophysical Sciences, University of Chicago, 5734 South Ellis Avenue, Chicago, IL 60637, USA

<sup>3</sup>Department of Paleontology, GNS Science, Lower Hutt 5040, New Zealand

<sup>4</sup>School of Geography, Environment and Earth Science, Victoria University of Wellington, Wellington 6140, New Zealand

<sup>5</sup>Lead Contact

\*Correspondence: rdbicknell@gmail.com

<https://doi.org/10.1016/j.isci.2018.09.013>



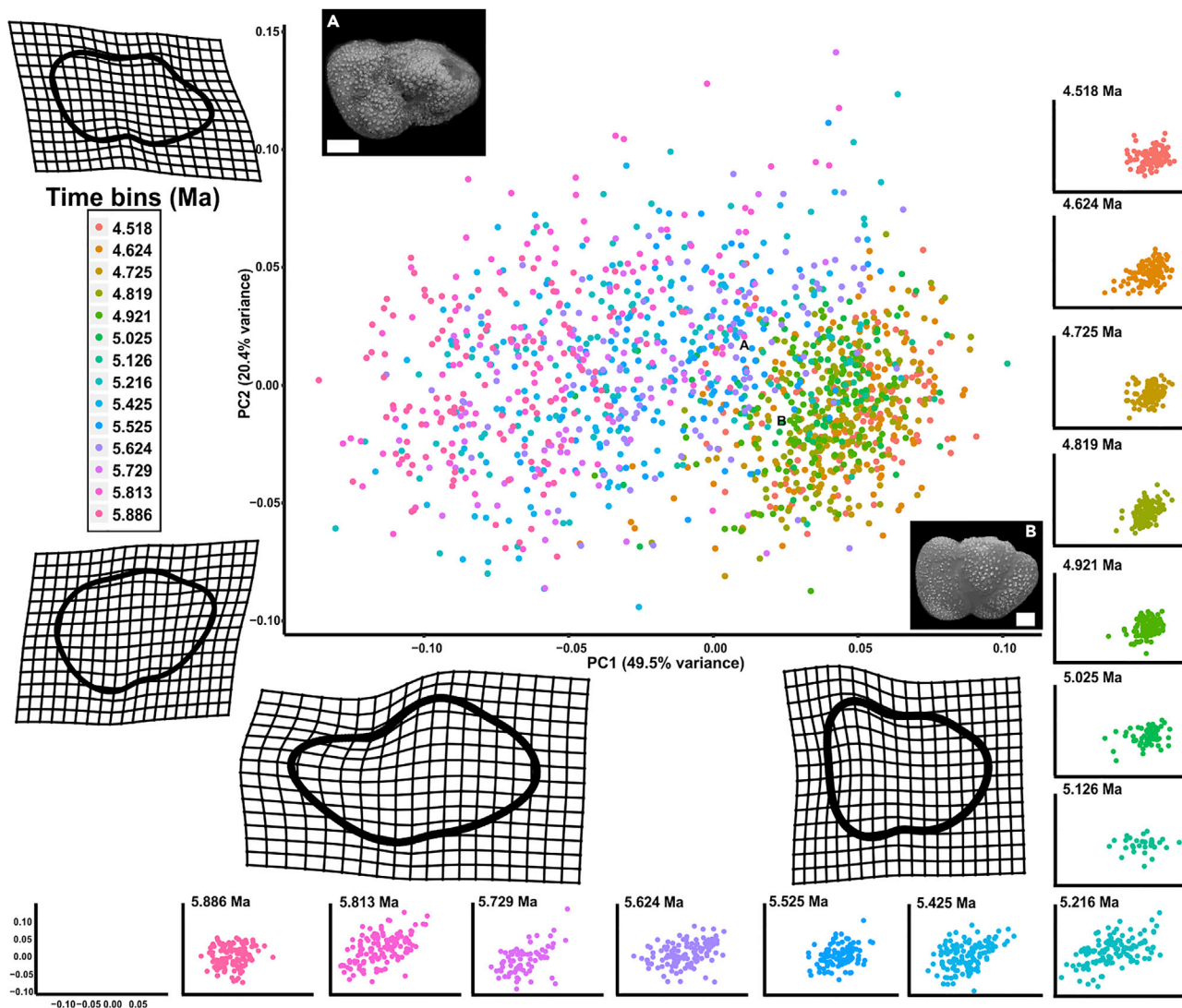


**Figure 1. Evolution of *Truncorotalia* in Principal Component Analysis Space**

Clusters migrate from negative to positive PC1 values across the studied intervals. This shift reflects a taxonomic change associated with the inflation of the final chamber and is typified by a large jump in morphology at about 5.1 Ma. Note that there is no time bin for 5.3 Ma due to the lack of specimens.

(A) *Truncorotalia juanai* specimen (Specimen FP5584).

(B) *Truncorotalia crassaformis* specimen (Specimen FP5583).

Scale bars: 50  $\mu$ m in (A and B). Scanning electron micrographs were taken using a JEOL JSM-6610LA at Victoria University of Wellington, under 15-kV and low vacuum. Specimens were not coated before imaging. Specimens are housed at GNS Science, Lower Hutt 5040, New Zealand.

contradict previous theories and preclude the need for an intermediate form along the transition (*sensu* Cifelli and Scott, 1986).

## RESULTS

Principal component (PC) 1, derived from a Procrustes-based geometric morphometric analysis, describes the degree of test ventral inflation (49.5% of total variance). *Truncorotalia crassaformis*, typically known from Pliocene deposits, has a more ventrally elevated final test chamber compared with the typically Miocene *T. juanai* (Cifelli and Scott, 1986). PC1 therefore defines the major differences between end members of the lineage across this temporal interval and is the most useful for understanding the evolutionary transition within *Truncorotalia* (Figure 1, outline reconstructions). The clusters in each time bin—specimens from sampled horizons in PC space—transition from negative PC1 space to positive PC1 space across the

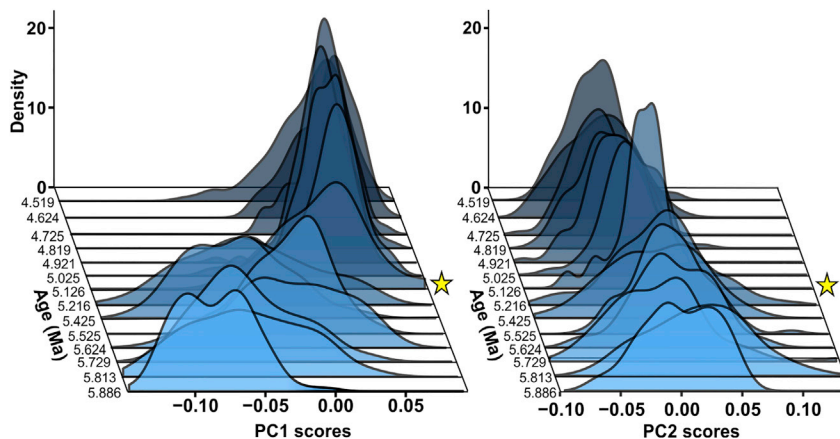


**Figure 2. Transitions of Truncorotalid Morphospace Defined by PC1 and PC2**

The transition from a diverse population of *Truncorotalia* to a constrained *Truncorotalia* population is most obvious at 5.1 Ma in PC1 and is present, but more subtle, in PC2. Stars indicate where the transition occurs.

studied interval. There is a jump at 5.1 Ma (Figure 1, time bin plots and Figure 2), which was equally documented in the time-series plots (Figures 3A and 3B). Furthermore, this shift in morphology is associated with a significant  $\sim 50\%$  decrease in the range of morphological variation (disparity) calculated as Procrustes variances (PV)— $PV_{5.216} = 0.0063$  to  $PV_{5.126} = 0.0033$  (PV distance = 0.003, p value = 0.001; Figure 3C). Overall, between 4.5 and 5.1 Ma disparity values are lower (PV ranges between 0.0021 and 0.0033) and points cluster closer in the PC space than between 5.1 and 5.9 Ma (PV ranges between 0.0038 and 0.0063). Timing of the transition to samples with constrained morphological variation reaffirms the suggested first-appearance datum of 5.1 Ma at Deep Sea Drilling Project (DSDP) Site 593 in Crundwell and Nelson (2007). PC2 tracks the change in test shape from more axially compressed to more axially expanded (20.4% of total variance), similar to the proposed changes in *Truncorotalia* noted in Arnold (1983) and Cifelli and Scott (1986).

The time-series analyses provide overwhelming evidence of a shift along PC1 (Figure 4A; Table S2). A comparison of nine models supports only an unbiased random walk to stasis shift model (Akaike weight [AW] = 0.916). All other models are rejected, including the generalized random walk model (AW = 0.012) needed to support a hypothesis of gradual phyletic change over time. Support values for PC2 also suggest a shift (Figure 4B), either between static intervals (i.e., PE model; AW = 0.512) or from an unbiased random walk to stasis (AW = 0.249). However, a simple unbiased random walk across the whole time series along PC2 also received some support compared with other models (AW = 0.127) (Table S3). No statistical support for bimodality in any time bin along PC1 and PC2 was found (Data S5).

## DISCUSSION

The origin of recent truncorotalid diversity is traced back to the evolutionary event documented across the Miocene/Pliocene boundary considered here (Kennett and Srinivasan, 1983; de Vargas et al., 1999; Boudagher-Fadel, 2012; Scott et al., 2015). *Truncorotalia crassaformis* evolved abruptly after the Miocene/Pliocene boundary from a contentious ancestral species (Hornibrook, 1981; Cifelli and Scott, 1986; Bylinskaya, 2004; Scott et al., 2015). Uncertainty regarding the ancestral taxon has arisen as the appearance of *T. crassaformis* has not been substantiated with a “well-authenticated evolutionary sequence” (Cifelli and Scott, 1986, p. 50). *T. juanai* (Scott et al., 1990; Crundwell and Nelson, 2007), *Hirsutella cibaoensis* (Arnold, 1983; Aze et al., 2011; Boudagher-Fadel, 2012), *T. crassula* (Kennett and Srinivasan, 1983), *Globorotalia aemiliana* (Colalongo and Sartoni, 1967; Lamb and Beard, 1972), *G. subscitula* (Blow, 1969), and a “nonspecialized scituline globorotalid” (Cifelli and Scott, 1986, p. 49) have all been suggested as possible ancestral taxa. Here we developed on Cifelli and Scott (1986) and others to support the thesis that *T. juanai* (= *H. cibaoensis* in Arnold (1983)) experienced a rapid evolutionary transition to the ventrally inflated *T. crassaformis*. This change lacked a transitional *T. crassaformis* population (i.e., metasppecies) along the temporal sequence, although it is characterized by a peak in disparity immediately before the transition where both *T. juanai* and *T. crassaformis* morphologies were present (Figures 1 and 4). Here we interpret

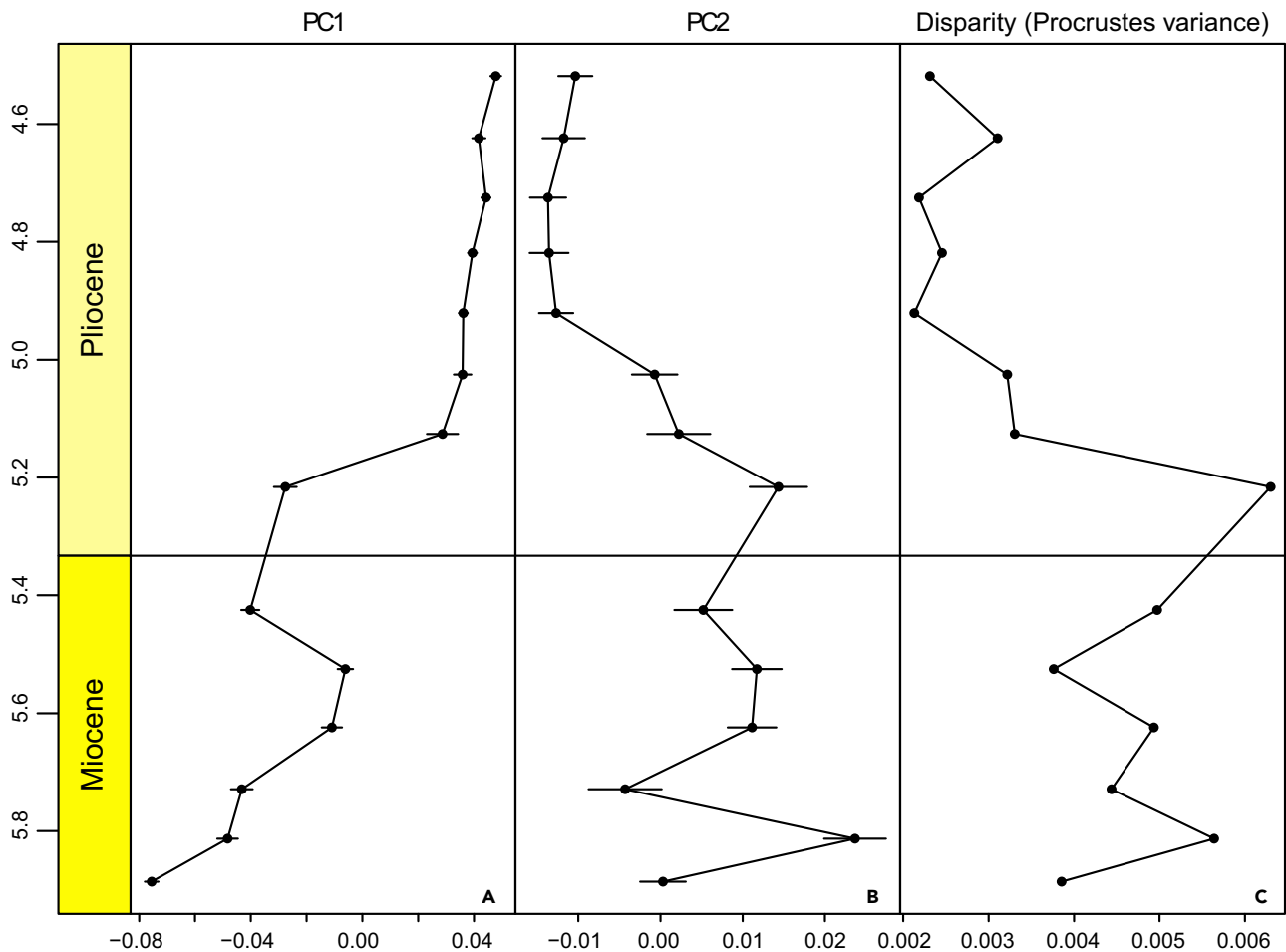


**Figure 3. Mean Morphology and Disparity of Truncorotalids across the Miocene/Pliocene**

(A) PC1 shows a jump from an unbiased random walk to stasis at 5.1–5.2 Ma. Error bars reflect the variance in each time-bin.

(B) PC2 shows a contemporaneous but less pronounced shift than PC1. PC2 is best described by a more punctuated model. Error bars reflect the variance in each time-bin.

(C) Disparity through time reveals an associated shift in the range of morphological variation at 5.1–5.2 Ma, demonstrating the rapid fixation of the novel morphology following the shift. Related to [Tables S1–S3](#).

the patterns within the context of two phyletic evolutionary theories, PE and QE, but acknowledge that extinction-survival dynamics cannot be precluded. This interpretation rejects the notion of a gradual transition along the *Truncorotalia* lineage proposed by [Arnold \(1983\)](#). Although [Arnold \(1983\)](#) documented an accelerated rate of evolution along the lineage in the early Pliocene, his broader interpretation was likely biased by the prevailing opinion at that time: that planktonic foraminiferal evolution was predominantly gradual ([Wei, 1987](#); [Wei and Kennett, 1988](#); [Aze et al., 2011](#)).

### Punctuated Equilibria

The theory of PE was presented by [Eldredge and Gould \(1972\)](#) as an alternative to phyletic gradualism and drove extensive research evaluating various evolutionary patterns and processes in the fossil record in search of evolutionary stasis (e.g., [Stanley, 1979](#); [Gingerich, 1985](#); [Turner and Paterson, 1991](#); [Jackson and Cheetham, 1999](#); [Hunt et al., 2015](#)). PE predicts that evolutionary dynamics can be described by long periods of stability that are punctuated by rapid pulses of change. Morphological variation accumulated within a lineage is therefore normally low, and the majority of variation is produced during rapid, episodic events ([Eldredge and Gould, 1972](#); [Eldredge et al., 2005](#)). These events occur so rapidly that they are seldom recorded in the fossil record ([Eldredge and Gould, 1972](#); [Eldredge et al., 2005](#)). The fundamental tenet of PE is therefore stasis. This feature of PE is difficult to define, and stasis is therefore generally

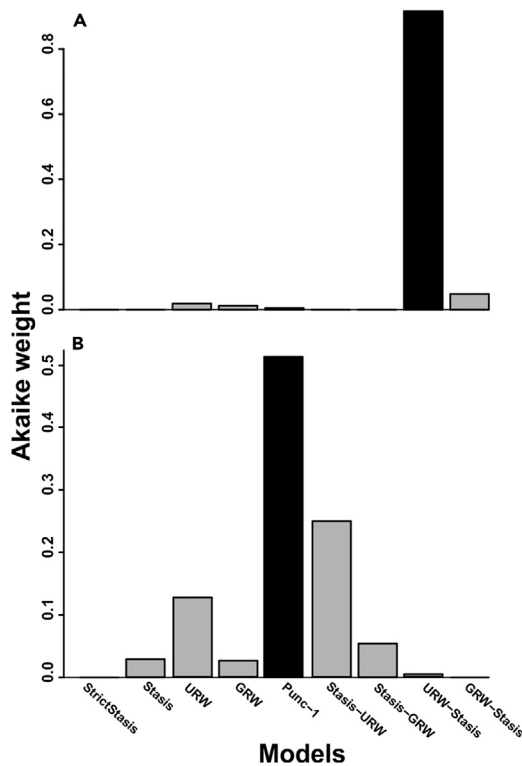


**Figure 4. Bar Plots of the Akaike Weights of the Nine Models**

(A) PC1 is best explained by a shift model of unbiased random walk to stasis.

(B) PC2 is best explained by punctuated equilibria model, although other models received some support. Black bars represent the best supported models.

referred to as “little to no net accrued species-wide morphological change” (Eldredge et al., 2005, p. 133). Mathematical definitions of stasis include (1) random variance over time, which assumes that the morphological conditions at one time interval are independent of those of the preceding or succeeding interval (“stasis” model of Hunt et al. (2015)), and (2) highly constrained variance that approaches zero (“strict stasis” model of Hunt et al., (2015)). Even unbiased random walks—variation in morphological change between intervals about a steady mean—can also describe little to no net change (Eldredge et al., 2005).

With these stipulations in mind, we posit that our results may conform to the predictions made by PE. This is especially the case for PC2, which recovers equivocal support for the “Punc-1” model of Hunt et al. (2015)—stasis before and after a shift. PC1 shows support for stasis after the transition and an unbiased random walk before the transition. This pattern does not conform to the traditional view of PE (Eldredge and Gould, 1972; Gould and Eldredge, 1977; Kirkpatrick, 1982); however, stasis as defined by Eldredge et al. (2005) could include the basic patterns characteristic of an unbiased random walk. *Truncorotalia* may have therefore experienced PE after the Miocene/Pliocene boundary.

### Quantum Evolution

Three decades before Eldredge and Gould’s contribution, George G. Simpson proposed QE: a rapid shift from one adaptive zone to another (Simpson, 1944, 1953). Simpson considered QE as one end member of a spectrum within phyletic evolution (i.e., ancestor-descendent relationships; Simpson, 1953) with phyletic gradualism at the other end. Simpson (1953) particularly viewed QE as the process by which higher taxonomic levels (such as families and orders) originated and associated the theory with the initial explosive phase of adaptive radiations. Although QE has been considered outdated, especially regarding the “evolution” of higher taxonomic ranks, it makes certain predictions about the nature of an evolutionary (quantum) shift that PE does not. QE therefore remains a viable explanation for evolutionary patterns and was even recently interpreted as a mechanism in the adaptive radiation of bird bills (Cooney et al., 2017). As such, we have highlighted this hypothesis as an alternative to PE.

The observed pattern of evolution from morphologies characteristic of *Truncorotalia juanai* to those of *T. crassaformis* could be explained as a quantum evolutionary shift along the planktonic foraminiferal

lineage given that we recover a rapid (tachytelic), “linear, but relatively short” (Simpson, 1944 p. 216), and “all-or-none” (Simpson, 1953 p. 389) transition from an ancestral morphology to a descendant morphology. The ancestral group—*T. juanai*—does not persist after *T. crassaformis* evolved (Simpson, 1944, 1953; Kirkpatrick, 1982). This “sharp shift from one position [morphology] to another” (Simpson, 1944, p. 216) is documented in Figure 2 and partly mirrors the idealized representation of QE presented in Simpson (1944, Figure 31) and Kirkpatrick (1982, Figure 3) and can certainly be interpreted within the phyletic evolution continuum of Simpson, 1953. Although aspects of this shift also conform to the stipulations of PE (see previous section), our results reveal that *T. juanai* was a morphologically diverse species during the Miocene before an evolutionary event in the Pliocene, where the descendant species became morphologically constrained (Kirkpatrick, 1982; Arnold, 1983; Cifelli and Scott, 1986) (Figure 3). Associated transitions between morphology and disparity are not explicitly required for PE, but are a stipulation of QE. Specifically, we recover “... relative instability with the system shifting toward an equilibrium not yet reached” and fluctuations in variation and a “new variant [that is] ... rapidly fixed” (Simpson, 1944; table 19). These dynamics support the idea that QE might explain the major and abrupt evolutionary shift within *Truncorotalia* after the Miocene/Pliocene boundary, perhaps in preference to PE.

One important expectation of QE remains difficult to infer: the shift after the Miocene/Pliocene boundary represents a transition from one adaptive zone to another. As described earlier, the morphological shift is associated with a ventral extension of the final test (Figures 1, 2, and 3). In Neogene planktonic foraminifera, ventrally extended test shapes are considered to be adaptations to better exploit oligotrophic waters, based on the observed distribution of ventrally inflated extant groups (Scott et al., 1990, 2015). Furthermore, extant *Truncorotalia* species are deep-water dwelling, ventrally inflated species that inhabit a deep thermocline (Hornibrook, 1981; Boudagher-Fadel, 2012). Selection for a subset of the *Truncorotalia* population about the Miocene/Pliocene boundary may therefore have produced a morphological stock capable of adapting to a deep-oceanic zone, eventually resulting in the recent truncorotalid diversity (de Vargas et al., 2001; Aze et al., 2011; Quillevère et al., 2011; Scott et al., 2015). Indeed, numerous studies have linked changes in planktonic foraminiferal morphology to shifts in adaptive zones and responses to environmental conditions (e.g., de Vargas et al., 1999; Quillevère et al., 2011). However, without comparisons to other lineages and a more detailed assessment of the paleoenvironments from DSDP Site 593, the driver(s) behind this transition and associated adaptive responses, if present, remains speculative.

### Future Directions

The first recorded appearance of *Truncorotalia crassaformis* in the fossil record is at 5.7 Ma (Aze et al., 2011), before the shift recognized here. Such a scenario would predict a bimodal distribution in older samples illustrating the co-existence of both species (*sensu* Scott, 2011), rejecting phyletic evolution, and supporting the extinction of *T. juanai* and survival of *T. crassaformis*. However, statistical tests for bimodality failed to reject unimodality in any time bin along PC1 and PC2 (Data S5). Furthermore, morphologies typical of *T. crassaformis* (positive PC1 and negative PC2 values; lower left quadrant) are exceedingly rare in horizons before the shift. Such morphologies account for a maximum of 13% of the population in any given Miocene sample, but account for ~27%–68% of populations in Pliocene samples (Table S4). These data both suggest that *Truncorotalia* populations during the Miocene exhibit high levels of disparity, sometimes even expanding the morphological gamut into regions similar to *T. crassaformis*. However, true *T. crassaformis* appear abruptly and are quickly fixed to a largely confined area of morphospace. Future research could expand the temporal scope of our analyses, older than 5.9 Ma, which may provide greater context for the onset of morphologies associated with *T. crassaformis*. Furthermore, a study using another DSDP site preserving material that spans 5.8–4.5 Ma and that is geographically separated from DSDP Site 593 could determine if the evolutionary event recovered here is general or localized (*sensu* Lazarus et al., 1995).

### Limitations of Study

Two uncertainties concerning the materials used here are noted. First, the evolutionary transition occurred at the change from DSDP Site Hole 593 to Hole 593A residues. Although unfortunate, this would not have impact on the recovered evolutionary patterns, as both holes were obtained from the same site (DSDP 593); were drilled less than 10 m apart, from the same longitude and latitude; and have been treated as duplications of each other by previous workers (Kennett and von der Borch, 1986). Despite their proximity, we cannot completely reject the possibility of a migratory event between the two holes. However, we view this option as unlikely as planktonic foraminifera are generally well distributed within major bodies of water

(Cifelli and Scott, 1986) and no major changes in oceanic waters masses occurred at DSDP Site 593 across the Miocene/Pliocene boundary (Nelson and Cooke, 2001). A further control on planktonic foraminiferal distribution is vertical niche partitioning within the water column (Seears et al., 2012). This partitioning would have allowed populations to be separated, but would not have prevented the record of *Truncorotalia crassaformis* at DSDP 593. As such, although a migration event is possible, it seems unlikely. As mentioned above, a study of another hole would help explore this issue further.

The second uncertainty is the notable loss of specimens between 5.2 and 5.3 Ma, before the shift. No typical *Truncorotalia* specimens are recovered from this interval, although rare, malformed individuals (i.e., specimens with aberrant morphologies) were found (Mancin and Darling, 2015). Although malformed individuals were not included in this study, as we wanted to assess the transition within a standard population, it is worth noting that malforms reflect stressed populations and an abiotic response to oceanic conditions (Mancin and Darling, 2015; Kontakiotis et al., 2016). Oceanic cooling at the terminal Miocene may have affected the *Truncorotalia* population, producing malforms, hinting at potential drivers behind the evolutionary events described here (Hornibrook, 1981; Malmgren and Berggren, 1987; Stanley et al., 1988; Lear et al., 2015).

## Conclusion

We documented and assessed the evolutionary transition along *Truncorotalia* across the Miocene/Pliocene boundary using semilandmark morphometrics and time-series analyses. A potentially localized and rapid evolutionary shift between two end members of *Truncorotalia*, *T. juanai* and *T. crassaformis*, at 5.1–5.2 Ma reveals that the evolutionary dynamics were not gradual and rejects the notion of an intermediate form along the lineage (contra Arnold, 1983; Cifelli and Scott, 1986). The transition between end members involved a major reduction in morphological diversity and a transition to a more constrained morphological stock. Furthermore, likelihood-based time-series analyses strengthen this hypothesis through rejection of simple gradual or random modes of evolution, in favor of shift models, which can be interpreted within the context of both Simpson's QE and Eldredge and Gould's PE. Through this study we hope to augment research into tempo and mode in planktonic foraminifera and highlight certain expectations of Simpson's theory, which are not explicit to PE. We envision that application of these methods by planktonic foraminiferal researchers will garnish further explicit tests of tempo and mode in this iconic fossil group.

## METHODS

All methods can be found in the accompanying [Transparent Methods supplemental file](#).

## SUPPLEMENTAL INFORMATION

Supplemental Information includes Transparent Methods, four tables, and six data files and can be found with this article online at <https://doi.org/10.1016/j.isci.2018.09.013>.

## ACKNOWLEDGMENTS

We thank Michael Knappertsbusch for training on AMOR. We thank Gene Hunt for his help with paleoTS. We thank George Scott, John Paterson, and Michael Knappertsbusch for useful discussion regarding this research. We thank Stephen Pates for reading an early draft of the manuscript. This research was funded by the William V. Sliter Research Award (2014) from the Cushman Foundation (R.D.C.B.) and the Australian Postgraduate Award (R.D.C.B.). Finally, we thank the two anonymous reviewers for their helpful comments, which improved the manuscript.

## AUTHOR CONTRIBUTIONS

R.D.C.B. and N.E.C. designed the study, collected/analyzed the data, interpreted the results, and wrote the manuscript. K.S.C. interpreted the morphological results. J.S.C., M.C., and M.H. conceived the project. All authors were involved in discussing the results and revising the manuscript.

## DECLARATION OF INTERESTS

The authors declare no competing interests.



Received: April 3, 2018

Revised: August 21, 2018

Accepted: September 14, 2018

Published: October 17, 2018

## REFERENCES

- Arnold, A.J. (1983). Phyletic evolution in the *Globorotalia crassaformis* (Galloway and Wissler) lineage: a preliminary report. *Paleobiology* 9, 390–397.
- Aze, T., Ezard, T.H., Purvis, A., Coxall, H.K., Stewart, D.R., Wade, B.S., and Pearson, P.N. (2011). A phylogeny of Cenozoic macroperforate planktonic foraminifera from fossil data. *Biol. Rev.* 86, 900–927.
- Belyea, P.R., and Thunell, R.C. (1984). Fourier shape analysis and planktonic foraminiferal evolution: the *Neogloboquadrina-Pulleniatina* lineages. *J. Paleontol.* 58, 1026–1040.
- Blow, W.H. (1969). Late Middle Eocene to Recent planktonic foraminiferal biostratigraphy. *Proceedings of the First International Conference on Planktonic Microfossils*. EJ Brill, pp. 199–422.
- Boudagher-Fadel, M.K. (2012). The Cenozoic Planktonic Foraminifera: The Neogene. *Biostratigraphic and Geological Significance of Planktonic Foraminifera* (Elsevier), pp. 199–260.
- Bylinskaya, M.E. (2004). Range and stratigraphic significance of the *Globorotalia crassaformis* plexus. *J. Iber. Geol.* 31, 51–64.
- Cifelli, R., and Scott, G. (1986). *Stratigraphic Record of the Neogene Globorotalid Radiation (Planktonic Foraminiferida)* (Smithsonian Institution Press).
- Colalongo, M.L., and Sartoni, S. (1967). *Globorotalia hirsuta aemiliana* nuova sottospecie cronologica del Pliocene in Italia. *Giornale Geol.* 34, 265–279.
- Collins, L.S. (1989). Evolutionary rates of a rapid radiation: the Paleogene planktic foraminifera. *Palaios* 4, 251–263.
- Cooney, C.R., Bright, J.A., Capp, E.J.R., Chira, A.M., Hughes, E.C., Moody, C.J.A., Nouri, L.O., Varley, Z.K., and Thomas, G.H. (2017). Mega-evolutionary dynamics of the adaptive radiation of birds. *Nature* 542, 344–347.
- Crundwell, M.P., and Nelson, C.S. (2007). A magnetostratigraphically-constrained chronology for late Miocene bolboformids and planktic foraminifers in the temperate Southwest Pacific. *Stratigraphy* 4, 1–34.
- Darwin, C. (1859). *On the Origin of the Species by Natural Selection* (John Murray).
- de Vargas, C., Renaud, S., Hilbrecht, H., and Pawlowski, J. (2001). Pleistocene adaptive radiation in *Globorotalia truncatulinoides*: genetic, morphologic, and environmental evidence. *Paleobiology* 27, 104–125.
- de Vargas, C., Norris, R., Zaninetti, L., Gibb, S.W., and Pawlowski, J. (1999). Molecular evidence of cryptic speciation in planktonic foraminifers and their relation to oceanic provinces. *Proc. Natl. Acad. Sci. USA* 96, 2864–2868.
- Depéret, C.J.J. (1907). *Les transformations du monde animal*, Ernest Flammarion.
- Eldredge, N., and Gould, S.J. (1972). Punctuated equilibria: an alternative to phyletic gradualism. In *Models in Paleobiology*, T.J.M. Schopf, ed. (Freeman Cooper and Company), pp. 82–115.
- Eldredge, N., Thompson, J.N., Brakefield, P.M., Gavrilits, S., Jablonski, D., Jackson, J.B., Lenski, R.E., Lieberman, B.S., McPeck, M.A., and Miller, W., III (2005). The dynamics of evolutionary stasis. *Paleobiology* 31, 133–145.
- Ezard, T.H., Aze, T., Pearson, P.N., and Purvis, A. (2011). Interplay between changing climate and species' ecology drives macroevolutionary dynamics. *Science* 332, 349–351.
- Frerichs, W.E. (1971). Evolution of planktonic foraminifera and paleotemperatures. *J. Paleontol.* 45, 963–968.
- Gingerich, P.D. (1985). Species in the fossil record: concepts, trends, and transitions. *Paleobiology* 11, 27–41.
- Gould, S.J., and Eldredge, N. (1977). Punctuated equilibria: the tempo and mode of evolution reconsidered. *Paleobiology* 3, 115–151.
- Hornibrook, N.d.B. (1981). *Globorotalia* (planktic Foraminiferida) in the late Pliocene and early Pleistocene of New Zealand. *New Zeal. J. Geol. Geophys.* 24, 263–292.
- Hsiang, A.Y., Elder, L.E., and Hull, P.M. (2016). Towards a morphological metric of assemblage dynamics in the fossil record: a test case using planktonic foraminifera. *Philos. Trans. R. Soc. B Biol. Sci.* 371, 20150227.
- Hunt, G. (2006). Fitting and comparing models of phyletic evolution: random walks and beyond. *Paleobiology* 32, 578–601.
- Hunt, G. (2007). The relative importance of directional change, random walks, and stasis in the evolution of fossil lineages. *Proc. Natl. Acad. Sci. USA* 104, 18404–18408.
- Hunt, G. (2008). Gradual or pulsed evolution: when should punctuational explanations be prepared? *Paleobiology* 34, 360–377.
- Hunt, G., and Carrano, M.T. (2010). Models and methods for analyzing phenotypic evolution in lineages and clades. *Special Papers of the Paleontological Society* 16, 245–269.
- Hunt, G., Hopkins, M.J., and Lidgard, S. (2015). Simple versus complex models of trait evolution and stasis as a response to environmental change. *Proc. Natl. Acad. Sci. USA* 112, 4885–4890.
- Jackson, J.B.C., and Cheetham, A.H. (1999). Tempo and mode of speciation in the sea. *Trends Ecol. Evol.* 14, 72–77.
- Kennett, J.P. and von der Borch, C. (1986). Site 593: challenger plateau. *Initial Reports of the Deep Sea Drilling Project*, 90, 551–651.
- Kennett, J.P., and Srinivasan, M. (1983). *Neogene planktonic foraminifera: A phylogenetic atlas* (Hutchinson Ross).
- Kirkpatrick, M. (1982). Quantum evolution and punctuated equilibria in continuous genetic characters. *Am. Naturalist* 119, 833–848.
- Kontakiotis, G., Antonarakou, A., Drinia, H., Mortyn, G., and Zarkogiannis, S. (2016). Eastern Mediterranean marine ecosystem monitoring through morphologically abnormal bio-indicators. *Rapp. Comm. Int. Mer Médit* 41, 57.
- Lamb, J.L., and Beard, J.H. (1972). Late Neogene Planktonic Foraminifers in the Caribbean, Gulf of Mexico, and Italian Stratotypes, vol. 57 (The University of Kansas Paleontological Contributions), pp. 1–104.
- Lazarus, D.B. (2011). The deep-sea microfossil record of macroevolutionary change in plankton and its study, vol. 358 (Geological Society, London, Special Publications), pp. 141–166.
- Lazarus, D., Hilbrecht, H., Spencer-Cervato, C., and Thierstein, H. (1995). Sympatric speciation and phyletic change in *Globorotalia truncatulinoides*. *Paleobiology* 21, 28–51.
- Lear, C.H., Coxall, H.K., Foster, G.L., Lunt, D.J., Mawbey, E.M., Rosenthal, Y., Sosdian, S.M., Thomas, E., and Wilson, P.A. (2015). Neogene ice volume and ocean temperatures: insights from infaunal foraminiferal Mg/Ca paleothermometry. *Paleoceanography* 30, 1437–1454.
- Malmgren, B., Berggren, W., and Lohmann, G. (1983). Evidence for punctuated gradualism in the Late Neogene *Globorotalia tumida* lineage of planktonic foraminifera. *Paleobiology* 9, 377–389.
- Malmgren, B.A., and Berggren, W.A. (1987). Evolutionary changes in some Late Neogene planktonic foraminiferal lineages and their relationships to paleoceanographic changes. *Paleoceanography* 2, 445–456.
- Malmgren, B.A., Kučera, M., and Ekman, G. (1996). Evolutionary changes in supplementary apertural characteristics of the late Neogene *Sphaeroidinella dehiscens* lineage (planktonic foraminifera). *Palaios* 11, 192–206.
- Mancin, N., and Darling, K. (2015). Morphological abnormalities of planktonic foraminiferal tests in the SW Pacific Ocean over the last 550ky. *Mar. Micropaleontol.* 120, 1–19.
- Nelson, C.S., and Cooke, P.J. (2001). History of oceanic front development in the New Zealand

sector of the Southern Ocean during the Cenozoic—a synthesis. *New Zeal. J. Geol. Geophys.* **44**, 535–553.

Pearson, P.N. (1993). A lineage phylogeny for the Paleogene planktonic foraminifera. *Micropaleontology* **39**, 193–232.

Pearson, P.N., and Ezard, T.H. (2014). Evolution and speciation in the Eocene planktonic foraminifer *Turborotalia*. *Paleobiology* **40**, 130–143.

Quillevère, F., Morard, R., Escarguel, G., Douady, C.J., Ujiie, Y., De Garidel-Thoron, T., and de Vargas, C. (2011). Global scale same-specimen morpho-genetic analysis of *Truncorotalia truncatulinoidea*: a perspective on the morphological species concept in planktonic foraminifera. *Palaeogeogr. Palaeoclimatol. Palaeoecol.* **391**, 2–12.

Scott, G.H. (2011). Holotypes in the taxonomy of planktonic foraminiferal morphospecies. *Mar. Micropaleontol.* **78**, 96–100.

Scott, G.H., Bishop, S., and Burt, B.J. (1990). Guide to some Neogene Globorotalids (Foraminifera) from New Zealand, New Zealand Geological Survey.

Scott, G.H., Ingle, J.C., McCane, B., Powell, C.L., and Thunell, R.C. (2015). *Truncorotalia crassaformis* from its type locality: comparison with Caribbean plankton and Pliocene relatives. *Mar. Micropaleontol.* **117**, 1–12.

Seeers, H.A., Darling, K.F., and Wade, C.M. (2012). Ecological partitioning and diversity in tropical planktonic foraminifera. *BMC Evol. Biol.* **12**, 54.

Simpson, G.G. (1944). *Tempo and Mode in Evolution* (Columbia University Press).

Simpson, G.G. (1953). *Major Features of Evolution* (Columbia University Press).

Stanley, S.M. (1979). *Macroevolution: Pattern and Process* (W. H. Freeman and Company).

Stanley, S.M., Wetmore, K.L., and Kennett, J.P. (1988). Macroevolutionary differences between the two major clades of Neogene planktonic foraminifera. *Paleobiology* **14**, 235–249.

Strotz, L.C., and Allen, A.P. (2013). Assessing the role of cladogenesis in macroevolution by integrating fossil and molecular evidence. *Proc. Natl. Acad. Sci. USA* **110**, 2904–2909.

Turner, A., and Paterson, H. (1991). Species and speciation: evolutionary tempo and mode in the fossil record reconsidered. *Geobios* **24**, 761–769.

Wei, K.-Y. (1987). Multivariate morphometric differentiation of chronospecies in the late Neogene planktonic foraminiferal lineage *Globoconella*. *Mar. Micropaleontol.* **12**, 183–202.

Wei, K.-Y., and Kennett, J.P. (1988). Phyletic gradualism and punctuated equilibrium in the late Neogene planktonic foraminiferal clade *Globoconella*. *Paleobiology* **14**, 345–363.

**ISCI, Volume 8**

**Supplemental Information**

**Evolutionary Transition in the Late Neogene**

**Planktonic Foraminiferal Genus *Truncorotalia***

**Russell D.C. Bicknell, Katie S. Collins, Martin Crundwell, Michael Hannah, James S. Crampton, and Nicolás E. Campione**

| Time bins | PC1 mean     | PC1 variation | PC2 mean     | PC2 variation | Number of specimens |
|-----------|--------------|---------------|--------------|---------------|---------------------|
| 4.5185    | 0.047824677  | 0.000434703   | -0.010357565 | 0.000507552   | 118                 |
| 4.624     | 0.041749406  | 0.000663263   | -0.011769851 | 0.000785937   | 118                 |
| 4.725     | 0.044311474  | 0.000312265   | -0.013678819 | 0.000582694   | 120                 |
| 4.819     | 0.039455399  | 0.000309778   | -0.013549356 | 0.00066271    | 118                 |
| 4.921     | 0.036157805  | 0.000304769   | -0.012696294 | 0.000518549   | 119                 |
| 5.025     | 0.035912368  | 0.000648122   | -0.00070798  | 0.000506534   | 66                  |
| 5.126     | 0.028714004  | 0.000937043   | 0.0022205    | 0.000442058   | 30                  |
| 5.216     | -0.027622986 | 0.001992911   | 0.014342546  | 0.001455831   | 119                 |
| 5.425     | -0.040181654 | 0.00124135    | 0.005203453  | 0.001464512   | 118                 |
| 5.525     | -0.006104463 | 0.000746298   | 0.011721271  | 0.000886289   | 97                  |
| 5.624     | -0.010927092 | 0.001594211   | 0.01113362   | 0.001051029   | 120                 |
| 5.729     | -0.04320383  | 0.001159867   | -0.004300164 | 0.001502031   | 76                  |
| 5.813     | -0.048301772 | 0.001659668   | 0.023662372  | 0.001701167   | 120                 |
| 5.886     | -0.075546774 | 0.000720687   | 0.000298733  | 0.000926812   | 120                 |

**Table S1: Summary of the data entered into paleoTS, related to Figure 3.**

| Model        | Ancestral state           | $\Theta 1$               | $\Theta 2$ | $\sigma^2$               | $\mu$              | $\omega$                 | Shift (time bin) | LogL        | AIC          | AW           |
|--------------|---------------------------|--------------------------|------------|--------------------------|--------------------|--------------------------|------------------|-------------|--------------|--------------|
| StrictStasis |                           | 0.019                    |            |                          |                    |                          |                  | -1700       | 3414         | 0.000        |
| Stasis       |                           | 0.002                    |            |                          |                    | 0.002                    |                  | 24.9        | -44.7        | 0.000        |
| URW          | -0.075                    |                          |            | 0.005                    |                    |                          |                  | 35.6        | -66.1        | 0.019        |
| GRW          | -0.075                    |                          |            | 0.004                    | 0.090              |                          |                  | 36.8        | -65.3        | 0.012        |
| Punc-1       |                           | -0.036                   | 0.039      |                          |                    | 0                        | 7                | 37.9        | -63.4        | 0.005        |
| Stasis-URW   |                           | -0.029                   |            | 0.001                    |                    | 0.012                    | 7                | 31.5        | -50.5        | 0.000        |
| Stasis-GRW   |                           | -0.029                   |            | 0.037                    | 0.031              | 0.001                    | 7                | 28.9        | -40.5        | 0.000        |
| URW-Stasis   | <b>-7.51<sup>-2</sup></b> | <b>3.98<sup>-2</sup></b> |            | <b>5.25<sup>-3</sup></b> |                    | <b>1.79<sup>-5</sup></b> | <b>7</b>         | <b>45.7</b> | <b>-73.9</b> | <b>0.916</b> |
| GRW-Stasis   | -7.51 <sup>-2</sup>       | 3.96 <sup>-2</sup>       |            | 5.07 <sup>-3</sup>       | 7.15 <sup>-2</sup> | 1.81 <sup>-5</sup>       | 7                | 46.0        | -68.0        | 0.048        |

**Table S2: Summary data from the paleoTS model fitting for PC1 to 3 significant figures, related to Figure 4.** Bold is the preferred model.  $\Theta 1$ =mean one,  $\Theta 2$ =mean 2,  $\sigma^2$ =step variance,  $\mu$ = step mean,  $\omega$ =trait variance. LogL=log likelihood, AIC= Akaike information criterion , AW=waited AIC values.

| Model         | Ancestral state | $\Theta$                      | $\Theta_2$                     | $\sigma^2$  | $\mu$         | $\omega$                      | Shift<br>(time<br>bin) | LogL        | AIC          | AW           |
|---------------|-----------------|-------------------------------|--------------------------------|-------------|---------------|-------------------------------|------------------------|-------------|--------------|--------------|
| StrictStasis  |                 | -0.004                        |                                |             |               |                               |                        | -40.6       | 83.6         | 0.000        |
| Stasis        |                 | $-8^{-5}$                     |                                |             |               | 0                             |                        | 42.6        | -80.2        | 0.029        |
| URW           | 0.001           |                               |                                | 0.002       |               |                               |                        | 44.1        | -83.1        | 0.127        |
| GRW           | 0.002           |                               |                                | 0.001       | -0.009        |                               |                        | 44.2        | -79.9        | 0.026        |
| <b>Punc-1</b> |                 | <b><math>8.98^{-3}</math></b> | <b><math>-8.99^{-3}</math></b> |             |               | <b><math>3.98^{-5}</math></b> | <b>7</b>               | <b>49.2</b> | <b>-85.9</b> | <b>0.512</b> |
| Stasis-URW    |                 | $1.03^{-2}$                   |                                | $6.06^{-4}$ |               | $8.38^{-5}$                   | 7                      | 48.5        | -84.5        | 0.249        |
| Stasis-GRW    |                 | $1.03^{-2}$                   |                                | $4.08^{-4}$ | $-2.07^{-02}$ | $9.12^{-5}$                   | 7                      | 49.4        | -81.4        | 0.054        |
| URW-Stasis    | 0.001           | -0.009                        |                                | 0.003       |               | 0                             | 7                      | 46.6        | -75.6        | 0.004        |
| GRW-Stasis    | 0.001           | -0.009                        |                                | 0.003       | 0.021         | 0                             | 7                      | 46.8        | -69.6        | 0.000        |

**Table S3: Summary data from the paleoTS model fitting for PC2 to 3 significant figures, related to Figure 4. Bold is the preferred model.  $\Theta_1$ =mean**

one,  $\Theta_2$ =mean 2,  $\sigma^2$ =step variance,  $\mu$ = step mean,  $\omega$ =trait variance. LogL=log likelihood, AIC= Akaike information criterion , AW=waited AIC values.

| <b>Time bin</b> | <b>Number of specimens</b> | <b>Forms typical of <i>T. crassaformis</i></b> | <b>Percentage abundance</b> |
|-----------------|----------------------------|--|-----------------------------|
| <b>4.5185</b>   | 118                        | 80   | 67.797                      |
| <b>4.6240</b>   | 118                        | 69   | 58.475                      |
| <b>4.7250</b>   | 120                        | 82   | 68.333                      |
| <b>4.8190</b>   | 118                        | 79   | 66.949                      |
| <b>4.9210</b>   | 119                        | 76   | 63.866                      |
| <b>5.0250</b>   | 66                         | 32   | 48.485                      |
| <b>5.1260</b>   | 30                         | 8  | 26.667                      |
| <b>5.2160</b>   | 119                        | 6  | 5.042                       |
| <b>5.4250</b>   | 118                        | 0  | 0                           |
| <b>5.5250</b>   | 97                         | 13   | 13.402                      |
| <b>5.6240</b>   | 120                        | 11   | 9.167                       |
| <b>5.7290</b>   | 76                         | 2  | 2.632                       |
| <b>5.8130</b>   | 120                        | 0  | 0                           |
| <b>5.8860</b>   | 120                        | 1  | 0.833                       |

**Table S4: Changes to abundance of forms typical of *Truncorotalia crassaformis* in morphospace, related to Figure 1 and Figure 2. The forms are very rare before 5.12 Ma (0-13.4%) and increase drastically in samples younger than 5.12 Ma (26.6-68.3%).**

## Transparent Methods

Samples were derived from washed core microfossil residues from Deep Sea Drilling Project (DSDP) Site 593—consisting of Hole 593 and Hole 593A—on the Lord Howe Rise (40°30'S, 167°40'E; Nelson et al., 1986; Cooke et al., 2008). Both holes were used due to limited material available from Hole 593 alone. Both cores were drilled continuously at the same site from the sea floor at the same time, so represent the same stratigraphic record (Kennett and Von Der Borch, 1986). The abundance of *Truncorotalia* specimens across the Miocene/Pliocene boundary made Holes 593 and 593A ideal for the study. DSDP 593 samples were assigned age values using a time calibration model proposed by Crundwell (see Cooke et al., 2008), which used planktonic foraminiferal bioevents to construct the model and was subsequently calibrated with palaeomagnetic records from DSDP Site 1123 and has been applied to DSDP 593 studies in provide age constraint (Crundwell, 2004; Crundwell and Nelson, 2007; Cooke et al., 2008). One residue every *ca.* 100 kyr between 4.5–5.9 Ma was selected using this time calibration and studied. Samples between 5.2–5.9 Ma were Hole 593 residues and samples between 4.5–5.1 Ma were Hole 593A residues. Correlation across the holes was achieved by identifying similarly aged samples about 5.2–5.1 Ma in both holes. Residues were sieved through 300 and 212 µm sieves (to minimize ontogenetic changes in morphology). Where possible, at least 100 standard specimens (no kummerforms, malformed or heavily encrusted specimens) of *Truncorotalia* with a pseudospinose surface ultrastructure and low slit-like apertures were sampled (see taxonomic notes in Scott et al., 1990; 2015; Crundwell and Nelson, 2007). Malformed specimens were not studied as such specimens may have impacted the proposed multivariate analyses and masked the evolutionary signal in question. Specimens were sampled at the genus level to assess change in the genus across the Miocene/Pliocene boundary. The changes in morphology were then linked to the two end member species: *T. juanai* and *T. crassaformis*. However, no species-levels assignments were



made during specimen selection; samples are meant to reflect the bulk of *Truncorotalia* at any given interval.

No standard *Truncorotalia* specimens were identified at 5.3 Ma. A total of 1459 specimens were used in this study. Individuals were mounted in axial view (the most informative view showing morphological change), orientated and imaged using the Automated Measurement System for Shell Morphology (Knappertsbusch et al., 2009; Mary and Knappertsbusch, 2013; 2015; Knappertsbusch, 2016). Outlines of specimen images, as  $xy$  coordinates, were gathered using the outlining method developed by Knappertsbusch et al. (2009). Outline files were converted into a semilandmark array in R (R Development Core Team, 2017) and outline points were resampled so that all specimens were represented by 200 semilandmarks whose final positions were determined by minimizing their bending energies in Generalized Procrustes Analysis (GPA; Supplementary File 1, Supplementary Data 1). Semilandmark analyses are a useful approach to study foraminiferal evolution, and outlines are the best representation of their morphology (Hull and Norris, 2009; Scott et al., 2015; Hsiang et al., 2016; Shi and Macleod, 2016). However, previous analyses have applied traditional morphometric approaches (e.g., linear measurements, counts of test chambers) and Geometric Morphometric techniques (e.g., Fourier and Eigenshape analyses) (Arnold, 1983; Belyea and Thunell, 1984; Healy-Williams, 1983; 1984; Wei, 1987; Malmgren et al., 1996). Procrustes Superposition and Principal Component Analysis (PCA) were run in the R package geomorph (Adams and Otárola-Castillo, 2013) and visualized through a scatter plot and density distributions (Supplementary Data 2, 3). Temporal variation along Principal Components (PCs) 1 and 2 data were analysed using likelihood-based time-series analyses implemented in the paleoTS package (the 'fit9models' function) to test between various models of evolution (Supplementary Tables 1–3) (Hunt, 2015). Only PCs 1 and 2 (69.9% of the total variance) were interpreted. Variance was not pooled for this analysis. Morphological

variation (i.e., disparity) across our interval was calculated as the Procrustes variance of the GPA-aligned data (Supplementary Data 4). As a result, it is a measure of total disparity and is not limited to specific axes of variation. Disparity was calculated through geomorph. Bimodality was assessed through Hartigan's Dip test for unimodality and analysed for all time bins for PCs 1 and 2 using the diptest package in R (Supplementary Data 5) (Maechler, 2016).

### **Supplemental References**

- Adams, D.C., and Otárola-Castillo, E. (2013). geomorph: an r package for the collection and analysis of geometric morphometric shape data. *Methods in Ecology and Evolution*, 4, 393–399.
- Cooke, P.J., Nelson, C.S., and Crundwell, M.P. (2008). Miocene isotope zones, paleotemperatures, and carbon maxima events at intermediate water-depth, Site 593, Southwest Pacific. *New Zealand Journal of Geology and Geophysics*, 51, 1–22.
- Crundwell, M.P. 2004. *New Zealand late Miocene biostratigraphy and biochronology – Studies of planktic foraminifers and bolboforms at oceanic Sites 593 and 1123, and selected onland sections*. PhD Thesis, University of Waikato, Hamilton, New Zealand.
- Crundwell, M.P., and Nelson, C.S. (2007). A magnetostratigraphically-constrained chronology for late Miocene bolboformids and planktic foraminifers in the temperate Southwest Pacific. *Stratigraphy*, 4, 1–34.
- Healy-Williams, N. (1983). Fourier shape analysis of *Globorotalia truncatulinoides* from late Quaternary sediments in the southern Indian Ocean. *Marine Micropaleontology*, 8, 1–15.
- Healy-Williams, N. (1984). Quantitative image analysis: Application to planktonic foraminiferal paleoecology and evolution. *Geobios*, 17, 425–432.

- Hull, P.M., and Norris, R.D. (2009). Evidence for abrupt speciation in a classic case of gradual evolution. *Proceedings of the National Academy of Sciences*, 106, 21224–21229.
- Hunt, G. (2015). paleoTS: Analyze Paleontological Time-Series. R package version 0.5-1.
- Knappertsbusch, M. (2016). Evolutionary prospection in the Neogene planktic foraminifer *Globorotalia menardii* and related forms from ODP Hole 925B (Ceara Rise, western tropical Atlantic): evidence for gradual evolution superimposed by long distance dispersal? *Swiss Journal of Palaeontology*, 135, 205–248.
- Knappertsbusch, M., Binggeli, D., Herzig, A., Schmutz, L., Stapfer, S., Schneider, C., Eisenecker, J., and Widmer, L. (2009). AMOR-A new system for automated imaging of microfossils for morphometric analyses. *Palaeontologia Electronica*, 12.
- Maechler, M. (2016). diptest: Hartigan's Dip Test Statistic for Unimodality - Corrected. R package version 0.75-7. <https://CRAN.R-project.org/package=diptest>.
- Mary, Y., and Knappertsbusch, M.W. (2015). Worldwide morphological variability in Mid-Pliocene menardellid globorotalids. *Marine Micropaleontology*, 121, 1–15.
- Mary, Y., and Knappertsbusch, M.W. (2013). Morphological variability of menardiform globorotalids in the Atlantic Ocean during Mid-Pliocene. *Marine Micropaleontology*, 101, 180–193.
- Nelson, C., Hendy, C., and Dudley, W. (1986). Quaternary isotope stratigraphy of Hole 593, Challenger Plateau, south Tasman Sea: preliminary observations based on foraminifers and calcareous nannofossils. *Initial reports of the Deep Sea Drilling Project*, 90, 1413–1424.
- R Development Core Team 2017. R: a language and environment for statistical computing. 3.3.3 ed. Vienna, Austria: R Foundation for Statistical Computing.

Shi, Y., and MacLeod, N. (2016). Identification of life-history stages in fusulinid foraminifera. *Marine Micropaleontology*, 122, 87–98.